Time-Domain Theoretical Analysis of the Noncoincidence Effect, Diagonal Frequency Shift, and the Extent of Delocalization of the C═O Stretching Mode of Acetone/Dimethyl Sulfoxide Binary Liquid Mixtures

Hajime Torii*

Department of Chemistry, School of Education, Shizuoka University, 836 Ohya, Shizuoka 422-8529, Japan

Maurizio Musso

Fachbereich Molekulare Biologie, Abteilung Physik und Biophysik, Universität Salzburg, Hellbrunnerstrasse 34, A-5020 Salzburg, Austria

Maria Grazia Giorgini

Dipartimento di Chimica Fisica ed Inorganica, Università di Bologna, Viale del Risorgimento 4, I-40136 Bologna, Italy

Received: May 16, 2005; In Final Form: July 4, 2005

A time-domain method for simulating vibrational band profiles that simultaneously takes into account both the diagonal and off-diagonal effects is developed and applied to the C═O stretching bands of neat liquid acetone and the acetone/dimethyl sulfoxide (DMSO) binary liquid mixtures. By using this method, it is possible to examine the influence of liquid dynamics on the noncoincidence effect (NCE), which arises from the off-diagonal vibrational interactions, as well as the frequency shifts and band broadening, which are related to both the diagonal and off-diagonal effects. It is shown that the simulations for the C═O stretching bands of acetone in acetone/DMSO binary liquid mixtures on the basis of this method can reproduce the experimentally observed concave curvature of the concentration dependence of the NCE and the unusually large frequency shift of the anisotropic Raman band. The widths of the infrared, isotropic Raman, and anisotropic Raman bands calculated for neat liquid acetone are also in good agreement with those observed. Based on these calculations, the extent of delocalization of the C═O stretching vibrational motions is examined by referring to two quantitative measures of this property, one calculated in the frequency domain and the other in the time domain. It is shown that the extent of delocalization gets larger as the mole fraction of acetone increases, the C═O stretching vibrations being delocalized over a few tens of molecules in neat liquid acetone. It is also shown that the extent of delocalization is related to the quantity called NCE detectability, which is the ratio between the magnitude of NCE and the bandwidth. It is therefore suggested that the extent of delocalization of vibrational motions may be estimated from observable features of Raman band profiles.

1. Introduction

Molecular vibrations in the liquid phase are affected by intermolecular interactions in various ways. The vibrational band profiles of the modes with large dipole derivatives are expected to show large effects from the intermolecular interactions related to those dipole derivatives,[1] such as the transition dipole coupling (TDC) between the vibrations of different molecules[2−4] and the frequency shifts due to the electric field-induced structural displacements.[5−10] The C═O stretching mode of acetone is a well-known example of such modes. It has been well recognized that this mode exhibits the noncoincidence effect (NCE),[11−15] i.e., the phenomenon that the frequency positions of the infrared (IR), isotropic Raman, and anisotropic Raman components of a vibrational band do not coincide. The magnitude of the NCE of this mode is $\tilde{\nu}_{\mathrm{NCE}}$ ($\equiv \tilde{\nu}_{\mathrm{aniso}} - \tilde{\nu}_{\mathrm{iso}}$) ≅ 5.2 cm^{-1} (ref 14), which is sufficiently large as compared with the bandwidth and is easily recognizable by measuring the polarized Raman spectrum. The NCE of this mode arises from the TDC between different molecules in the liquid,[2−4] which is classified as the "off-diagonal" effect in the vibrational exciton picture.[16] The fact that the NCE of this mode arises from the off-diagonal effect is experimentally proved by the isotopic and chemical dilution measurements,[14,17−19] in which the magnitude of the NCE is reduced as the concentration of acetone decreases and becomes vanishingly small for very dilute solutions. In the isotopic dilution measurements, in which the environment around molecules does not change in a chemical sense, it is theoretically predicted that almost all the changes in the magnitude of the NCE arise from the frequency shift of the isotropic Raman component.[20] This is supported by the measurements for the mixtures of the ^{12}C═O and ^{13}C═O species of liquid acetone done at 280 K,[19] in which the isotropic component of the ^{12}C═O stretching Raman band shifts from 1709 to 1715 cm^{-1} as the mole fraction of acetone-^{12}C decreases from 1.0 to ∼0.04, while the anisotropic component stays at 1715 cm^{-1} over the whole concentration range.

* Address correspondence to this author. Phone: +81-54-238-4624. Fax: +81-54-237-3354. E-mail: torii@ed.shizuoka.ac.jp.

10.1021/jp052565t CCC: $30.25
Published on Web 08/09/2005

In our recent experimental study[21] on the acetone/dimethyl sulfoxide (DMSO) binary liquid mixtures done at 293 K, however, it has been observed that the anisotropic component of the C═O stretching Raman band shows a shift from 1715 cm^{-1} in the neat liquid to 1710 cm^{-1} at the mole fraction of acetone-^{12}C of 0.1, while the isotropic component remains at almost the same frequency position at around 1710 cm^{-1}. It has been suggested that this result is reasonably explained by taking into account both the diagonal (environmentally induced) and off-diagonal (intermolecular vibrational coupling) effects.[21] According to this scheme, the isotropic component remains at almost the same frequency position because of the cancellation between the upshifting off-diagonal effect and the downshifting diagonal effect upon dilution in DMSO. We can observe a low-frequency shift for the anisotropic component, because there is essentially no frequency shift due to the off-diagonal effect for this component.

The downshifting diagonal effect described above arises from the difference between the acetone−acetone and acetone−DMSO intermolecular interactions. Since the chemical environment around acetone molecules changes as time evolves in a liquid mixture, the diagonal effect also induces band broadening as well as frequency shifts. In this case, because the motional narrowing effect[22] is expected, it is necessary to use a time-domain simulation method to do realistic simulations of the changes in the band profiles. Simulations with both the diagonal and off-diagonal effects simultaneously taken into account are interesting in that these two effects compete with each other in determining the extent of delocalization of vibrational modes.[23] This is also related to the efficiency of the vibrational excitation transfer that one can experimentally observe[24,25] in a time-domain measurement.

In the present study, for the purpose described above, the time-domain method for simulating the NCE previously developed[26] is extended to include the diagonal effect. By using this method, simulations on the C═O stretching mode in neat liquid acetone and the acetone/DMSO binary liquid mixtures are carried out. To specify the mechanism of the diagonal frequency shift arising from the difference between the acetone−acetone and acetone−DMSO intermolecular interactions, ab initio molecular orbital (MO) calculations are also carried out for some cluster species. From these calculations, the extent of delocalization of vibrational modes and its manifestation in the Raman spectral profiles of neat liquid acetone and the acetone/DMSO binary liquid mixtures are discussed.

2. Theoretical Formulation and Computational Procedure

A. Extended MD/TDC/WFP Method. In a previous study,[26] a time-domain method for simulating the influence of liquid dynamics on the NCE, called the MD/TDC/WFP method, has been developed by one of the present authors (HT). The formulation is briefly described as follows. For the Raman spectrum related to the *pq* element of the polarizability operator α_{pq} (where $p, q = 1, 2, 3$ corresponds to the *x*, *y*, and *z* axes of the liquid system), an important quantity is the wave function of the Raman excitation at time *t*, expressed as

$$|\psi_{pq}^{(R)}(t)\rangle = \exp_+\left[-\frac{i}{\hbar}\int_0^t d\tau\, H(\tau)\right]|\psi_{pq}^{(R)}(0)\rangle \qquad (1)$$

where

$$|\psi_{pq}^{(R)}(0)\rangle = \sum_{\xi=1}^{N}|\xi_0\rangle\langle\xi_0|\alpha_{pq}|0\rangle \qquad (2)$$

is the wave function formed by the Raman excitation at time $t = 0$, expressed by the wave function of the ground state $|0\rangle$, the polarizability operator α_{pq}, and the eigenstate $|\xi_0\rangle$ (numbered by ξ) of the liquid system at time $t = 0$. Here, *N* is the number of molecules participating in the vibrational band in question (the number of acetone molecules in the present study). $H(\tau)$ is the vibrational Hamiltonian, which is time-dependent because of the influence of the liquid dynamics. Due to this time dependence, a time-ordered exponential (denoted as $\exp_+$)[27] is involved in eq 1. By using the wave function $|\psi_{pq}^{(R)}(t)>$ and assuming $\hbar\omega \gg kT$, the Raman spectrum $I_{pq}^{(R)}(\omega)$ is expressed as

$$I_{pq}^{(R)}(\omega) = \mathrm{Re}\int_0^\infty dt\, \exp(i\omega t)\langle\langle 0|\alpha_{pq}|\psi_{pq}^{(R)}(t)\rangle\rangle \qquad (3)$$

where the large bracket stands for statistical average. The isotropic and anisotropic components of the Raman spectrum are obtained from appropriate combinations of $I_{pq}^{(R)}(\omega)$ with $p, q = 1, 2, 3$.

To calculate the time evolution of the vibrational wave function shown in eq 1, it is necessary to treat it as the product of short-time evolutions assuming that the Hamiltonian is essentially invariant during a very short time period, which is taken as equal to the time step of the molecular dynamics (MD) simulations. We obtain

$$|\psi_{pq}^{(R)}(\tau+\Delta\tau)\rangle = \exp\left[-\frac{i}{\hbar}\Delta\tau\, H(\tau)\right]|\psi_{pq}^{(R)}(\tau)\rangle = \sum_{\xi=1}^{N}|\xi_\tau'\rangle\exp[-i\omega_\xi(\tau)\Delta\tau]\langle\xi_\tau|\psi_{pq}^{(R)}(\tau)\rangle \qquad (4)$$

where $\omega_\xi(\tau)$ is the vibrational frequency for the eigenstate $|\xi_\tau\rangle$ at time τ, and $|\xi_\tau'\rangle$ is the wave function with the same amplitudes of molecular vibrations as $|\xi_\tau\rangle$ but with the molecular orientations evaluated at time $\tau + \Delta\tau$. We construct $H(\tau)$ every time step, diagonalize this Hamiltonian to get $\omega_\xi(\tau)$ and $|\xi_\tau\rangle$, and calculate the time evolution of vibrational excitations according to eq 4.

IR spectra are calculated in a similar way. An important quantity is the wave function of the IR excitation at time *t*, expressed as

$$|\psi_p^{(IR)}(t)\rangle = \exp_+\left[-\frac{i}{\hbar}\int_0^t d\tau\, H(\tau)\right]|\psi_p^{(IR)}(0)\rangle \qquad (5)$$

where

$$|\psi_p^{(IR)}(0)\rangle = \sum_{\xi=1}^{N}|\xi_0\rangle\langle\xi_0|\mu_p|0\rangle \qquad (6)$$

is the wave function formed by the IR excitation at time $t = 0$, and μ_p is the *p*th element of the dipole operator ($p = 1, 2, 3$). The time evolution of $|\psi_p^{(IR)}(t)\rangle$ is also calculated by treating it as the product of short-time evolutions in the same way as in eq 4. By using this wave function, the IR spectrum $I_p^{(IR)}(\omega)$ is expressed as

$$I_p^{(IR)}(\omega) = \mathrm{Re}\int_0^\infty dt\, \exp(i\omega t)\langle\langle 0|\mu_p|\psi_p^{(IR)}(t)\rangle\rangle \qquad (7)$$

In the MD/TDC/WFP method, the off-diagonal elements of the vibrational Hamiltonian $H(\tau)$ are determined by the TDC mechanism. Since the TDC constants depend on the locations and orientations of molecules and are therefore affected by the liquid dynamics, $H(\tau)$ is treated as time dependent. In the present

study, this method is extended to include the variation in the diagonal elements of $H(\tau)$ arising from the inhomogeneity of the microscopic environment of molecules and its changes due to the liquid dynamics. From the results of the ab initio MO calculations for molecular clusters described below in sections 2B and 3A, it is reasonable to treat the diagonal elements of $H(\tau)$ as controlled by the electric field from the surrounding molecules. This mechanism is expressed for the shift Δk_i in the quadratic force constant as[7,8,28]

$$\Delta k_i = \left(\frac{f_i}{k_i} \frac{\partial \boldsymbol{\mu}_i}{\partial q_i} - \frac{\partial^2 \boldsymbol{\mu}_i}{\partial q_i^2} \right) \mathbf{E}_i \qquad (8)$$

where k_i and f_i are the diagonal quadratic and cubic force constants for the vibration of the ith molecule (denoted as q_i), and $\mathbf{E}_i$ is the electric field operating on the ith molecule from the surrounding molecules. The first and second terms represent the effects of the mechanical and electrical anharmonicities on Δk_i.

In the present study, we assumed k_i (unperturbed value) to be $6.2637 \times 10^{-5}\ E_h\ a_0^{-2}\ m_e^{-1}$ (=1.7777 mdyn Å^{-1} amu^{-1}),[29] which corresponds to the vibrational frequency of 1737 cm^{-1} of the C═O stretching mode of acetone in the gas phase,[30] and the ratio $f_i/k_i = -2.7380 \times 10^{-2}\ a_0^{-1}\ m_e^{-1/2}$ was taken from the result of the ab initio MO calculation for an isolated acetone molecule at the MP3/6-31+G(2df,p) level. The magnitude of the dipole derivative was assumed to be $|\partial \boldsymbol{\mu}_i/\partial q_i| = 1.0143 \times 10^{-2}$ e $m_e^{-1/2}$ (=2.08 D Å^{-1} amu$^{-1/2}$) as in the previous study,[4] which is close to the calculated value of 1.0015×10^{-2} e $m_e^{-1/2}$ at the MP3/6-31+G(2df,p) level. The magnitude of the dipole second derivative, $|\partial^2 \boldsymbol{\mu}_i/\partial q_i^2| = 8.5574 \times 10^{-5}$ e $a_0^{-1}\ m_e^{-1}$, was taken from the calculation at the MP3/6-31+G(2df,p) level. The two derivatives are directed in the opposite direction along the C═O bond, so that the first and second terms of eq 8 partially cancel each other. They were assumed to be of fixed magnitudes as indicated above (i.e., neglecting the modulations of these magnitudes by the liquid dynamics), located at the center of the C═O bond, and the interactions with the electric field originating from the surrounding molecules were calculated. The dipole derivative was also used for calculating the off-diagonal force constants according to the TDC mechanism, and for evaluating the brackets that involve the dipole operator in eqs 6 and 7. The polarizability operator in eqs 2 and 3 was assumed to be axially symmetric with respect to the C═O bond of each molecule.

To calculate the electric field operating between molecules, the partial charges of atomic sites were determined by fitting to the electrostatic potentials around isolated molecules. From the calculations at the MP3/6-31+G(2df,p) level, they were determined as $q(C) = 0.46328$ e, $q(O) = -0.50524$ e, $q(CH_3) = 0.02098$ e for acetone, and $q(S) = 0.05996$ e, $q(O) = -0.42210$ e, $q(CH_3) = 0.18107$ e for DMSO. The methyl groups were treated as united atoms, and the charges were assumed to be located at the carbon atoms of these groups.

The MD simulations were performed by combining the above atomic charges with the Lennard-Jones parameters taken from previous studies.[31,32] Four-dimensional vectors (quaternions) were used to represent molecular orientations in solving the equations of motion, in combination with the leapfrog integration method.[33,34] The liquid systems consisted of 128 molecules in total, and the mole fraction of acetone was set as $x_{acetone} = 1.0$, 0.8, 0.6, 0.4, and 0.2. The volume of the cubic simulation cell was fixed so that the molecular volumes are equal to $v_{acetone} = 122.04$ Å^3 (ref 35) and $v_{DMSO} = 117.84$ Å^3 (ref 36). The temperature was kept at 293 K by adjusting the total kinetic energy every 200 fs. The time step was set to 2 fs. At each concentration, the system was equilibrated for about 2 ns, after which the production runs were carried out.

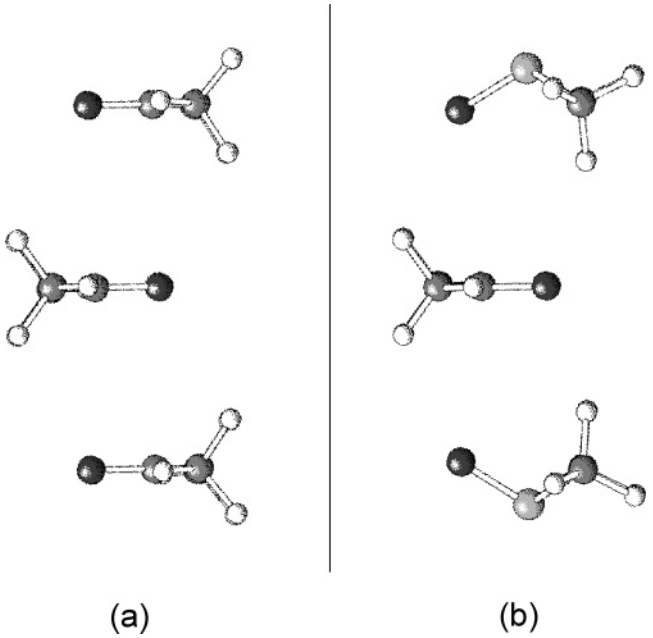

Figure 1. Structures (sideviews) of (a) the acetone trimer and (b) the acetone−$(DMSO)_2$ cluster in the antiparallel configuration calculated at the HF/6-31+G(2df,p) level.

To obtain a frequency resolution of about 0.5 cm^{-1} for the spectra calculated as Fourier transforms in eqs 3 and 7, the wave functions of vibrational excitation were calculated for about 65.5 ps (32 768 time steps). To get a good statistical average, the calculations were carried out for about 1300 samples at each concentration (about 2700 samples for $x_{acetone} = 0.2$), with the "time $t = 0$" of each sample being separated from that of another by more than 30 ps.

As a reference to the above calculations, the IR and Raman spectra in the static case were also calculated. Those spectra were obtained by freezing all the liquid dynamics in the calculations of the IR and Raman spectra, i.e., by using the MD/TDC method developed previously[4,16] but with the diagonal effect taken into account according to eq 8.

The simulations based on eqs 1−8 described above as well as the supplementary analyses described below in section 3C were carried out on a Hewlett-Packard zx6000 workstation with our original programs.

B. MO Calculations for Molecular Clusters. To specify the mechanism of the diagonal frequency shift arising from the difference between the acetone−acetone and acetone−DMSO intermolecular interactions, ab initio MO calculations were carried out for the acetone trimer and the acetone−$(DMSO)_2$ cluster in the antiparallel configuration shown in Figure 1 (sideview), as well as an isolated acetone molecule as a reference, at the HF/6-31+G(2df,p) level. For all these species, the vibrational frequencies (and the force constants) were calculated after the structure was fully optimized. For the acetone−$(DMSO)_2$ cluster, the diagonal force constant (in the vibrational exciton picture) was directly obtained from the frequency of the C═O stretching normal mode. However, this is not the case for the acetone trimer, since the C═O stretching normal modes of this cluster are delocalized due to the off-diagonal vibrational coupling. To extract the diagonal force constant for the central acetone molecule in this cluster, the

TABLE 1: Calculated Vibrational Frequencies and the Resulting Shift Δk of the Force Constant of the C═O Stretching Mode of Acetone Molecules in Different Environments and the Magnitude of the Electric Field E on the Center of the C═O Bond[a]

species and location	freq/cm^{-1}	Δk/mdyn Å^{-1} amu^{-1}	$E/10^{-2}$ E_h e^{-1} a_0^{-1}	Δk(estimated from E)[c]/ mdyn Å^{-1} amu^{-1}
isolated	1984.30			
acetone trimer, center[b]	1951.96	−0.0751	0.9465	−0.0726
acetone-$(DMSO)_2$ cluster	1937.64	−0.1079	1.4822	−0.1137

[a] Calculated at the HF/6-31+G(2df,p) level. [b] The vibrational frequency and the vibrational force constant for the molecule in the center are extracted by the average partial vector method. [c] By using eq 8. See text.

average partial vector (APV) method[10] was employed. A detailed explanation of this method has been given in a previous study[10] dealing with the case of the clusters of *N*-methylacetamide as an example.

To see how the shift in the diagonal force constant is related to the electric field from the surrounding molecules, the latter quantity was also evaluated by the ab initio MO method. For this purpose, the target molecule was removed, the positions of all the other molecules being fixed to those of the optimized structure of the original cluster, and the electric field was calculated at the specified position where the target molecule was located. In the present study, the electric field at the center of the C═O bond of the central acetone molecule was calculated for the acetone trimer and the acetone−$(DMSO)_2$ cluster.

The ab initio MO calculations described above (including those at the MP3/6-31+G(2df,p) level described in section 2A) were performed by using the Gaussian 98 program[37] on a Fujitsu VPP5000 supercomputer at the Research Center for Computational Science of the National Institutes of Natural Sciences at Okazaki. The vibrational analyses based on the APV method were carried out on a Compaq XP1000 workstation with our original programs.

3. Results and Discussion

A. Relation between the Diagonal Frequency Shift and the Electric Field in Molecular Clusters. The (unscaled) vibrational frequencies of the C═O stretching mode calculated for isolated acetone, the acetone trimer, and the acetone−$(DMSO)_2$ cluster are shown in the second column in Table 1. For the acetone trimer, the frequency corresponding to the diagonal force constant of the central molecule is extracted by using the APV method. It is clearly seen that the acetone−DMSO interaction gives rise to a larger frequency shift than the acetone−acetone interaction, in agreement with the result obtained from the experiment on the liquid mixtures.[21] The larger frequency shift for the acetone−DMSO interaction cannot be sufficiently well reproduced by using the dielectric continuum model with the self-consistent reaction field (SCRF) method.[38] As shown in our previous paper,[21] the C═O stretching frequency of acetone is calculated as 1961.87 and 1960.74 cm^{-1} in a dielectric medium of $\epsilon = 20.7$ (acetone) and 46.7 (DMSO), respectively. This result suggests that the molecular aspect of the solvent effect is important for reproducing the frequency shift of the C═O stretching mode of acetone. As compared with the observed frequency difference of 5.6 cm^{-1}, the calculated frequency difference of 14.3 cm^{-1} between the two clusters shown in Table 1 may seem to be too large. In fact, this is due to the fact that the ab initio MO calculations are done only for the clusters at their potential energy minima. By taking into account the thermal distributions, we can obtain a value in better agreement with the experimental result, as shown below in section 3B.

As shown in the fourth column in Table 1, the electric field at the center of the C═O bond of the central acetone molecule is calculated as 0.9465×10^{-2} and 1.4822×10^{-2} E_h e$^{-1}a_0^{-1}$, respectively, for the acetone trimer and the acetone−$(DMSO)_2$ cluster. By using eq 8 with the quadratic and cubic force constants ($k = 8.1746 \times 10^{-5}$ E_h a_0^{-2} m_e^{-1}, $f = -2.1706 \times 10^{-6}$ E_h a_0^{-3} $m_e^{-3/2}$) and the dipole first and second derivatives ($\partial\mu/\partial q = 1.2342 \times 10^{-2}$ e $m_e^{-1/2}$, $\partial^2\mu/\partial q^2 = -5.7508 \times 10^{-5}$ e a_0^{-1} m_e^{-1}) calculated at the HF/6-31+G(2df,p) level, it is possible to estimate the shift in the force constant Δk from the magnitude of the electric field. The result is shown in the fifth column in Table 1. It is clearly seen that the values of Δk thus estimated are in good agreement with those in the third column, which correspond to the frequency shifts in the second column. This result suggests that the diagonal frequency shifts of the C═O stretching mode of acetone arising from the interactions with the surrounding acetone and DMSO molecules are controlled by the electric field from those surrounding molecules. With the values of the quadratic and cubic force constants and the dipole first and second derivatives shown above, the contribution of the first term in eq 8 is 5 or 6 times larger than that of the second term. Therefore, it may be said that, in agreement with ref 39, the large modulation of the diagonal force constant of the C═O stretching mode of acetone by the electric field from the surrounding molecules is mainly due to the large dipole (first) derivative of this mode, and the mechanical anharmonicity is more effective than the electrical anharmonicity.

B. Noncoincidence Effect and Band Profiles. The IR, isotropic Raman, and anisotropic Raman spectra in the C═O stretching region calculated for neat liquid acetone and the acetone/DMSO binary liquid mixtures of $x_{acetone} = 1.0$, 0.8, 0.6, 0.4, and 0.2 by using the extended MD/TDC/WFP method are shown in Figure 2. The spectra calculated for different mole fractions are normalized with respect to the integrated intensities. At $x_{acetone} = 1.0$, the profiles of the three spectra are significantly different from each other because of the off-diagonal vibrational coupling, but they become similar to each other upon dilution in DMSO. The first moments of these spectra are plotted as functions of mole fraction in Figure 3a. It is clearly seen that the anisotropic Raman band shows a low-frequency shift upon dilution in DMSO, while the isotropic Raman band remains at almost the same frequency position, in agreement with the experimental result.[21] For all the bands, the calculated absolute frequency positions are higher than those observed by about 6 cm^{-1}. This may be due to the neglect of the electronic polarization effect in the treatment of the diagonal frequency shift in the present study, and/or due to the remaining errors in the parameters (dipole second derivatives, etc.) taken from the calculations at the MP3/6-31+G(2df,p) level. We suppose that the electronic polarization effect induces a low-frequency shift rather uniformly over the whole concentration range.

The gradient of the calculated frequency shift in Figure 3a is 6.0 cm^{-1} for the IR and 4.9 cm^{-1} for the anisotropic Raman band, in agreement with the observed frequency shift[21] of 5.6 cm^{-1} for the anisotropic Raman band. As discussed in section

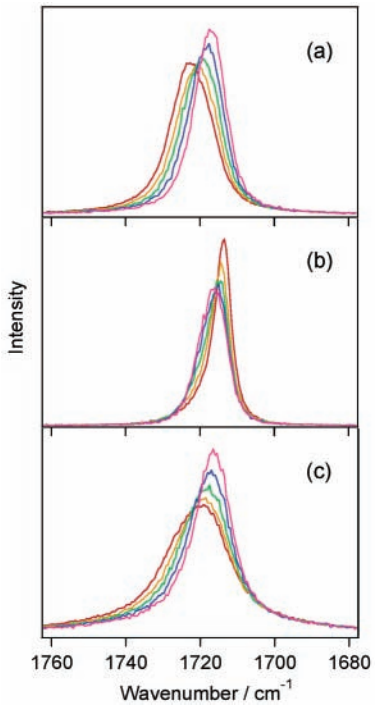

Figure 2. (a) IR, (b) isotropic Raman, and (c) anisotropic Raman spectra of neat liquid acetone and the acetone/DMSO binary liquid mixtures in the C═O stretching region calculated by the extended MD/TDC/WFP method. Red: $x_{acetone} = 1.0$ (neat liquid acetone). Orange: $x_{acetone} = 0.8$. Green: $x_{acetone} = 0.6$. Blue: $x_{acetone} = 0.4$. Purple: $x_{acetone} = 0.2$.

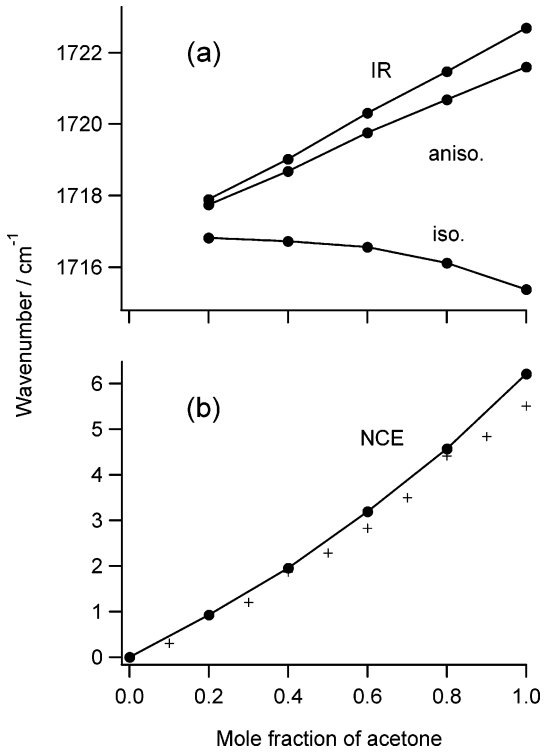

Figure 3. Concentration dependence of (a) the frequency positions of the IR, isotropic Raman, and anisotropic Raman bands (first moments of the band profiles) and (b) the magnitude of the NCE of the C═O stretching mode of acetone, calculated for neat liquid acetone and the acetone/DMSO binary liquid mixtures by the extended MD/TDC/WFP method (filled circles connected by solid lines). In part b, the observed values (averaged) taken from ref 21 (represented by "+") are also shown for comparison. Note that the observed value at $x_{acetone} = 0.2$ overlaps with the calculated value, so that the symbol for the former is not visible at this mole fraction.

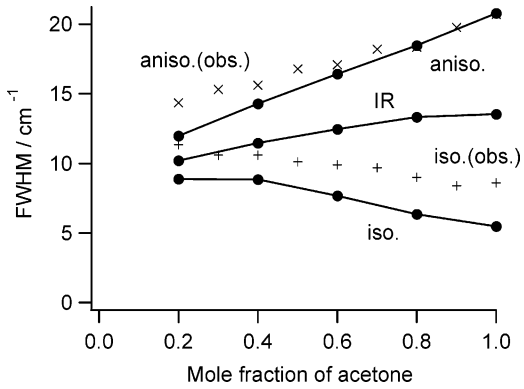

Figure 4. Concentration dependence of the full width at half-maximum of the IR, isotropic Raman, and anisotropic Raman bands of the C═O stretching mode of acetone, calculated for neat liquid acetone and the acetone/DMSO binary liquid mixtures by the extended MD/TDC/WFP method (filled circles connected by solid lines) and observed experimentally (+ and ×). Note that the observed values for the anisotropic Raman band at $x_{acetone} = 1.0$ and 0.8 overlap with the calculated values.

3A, these values are smaller than the frequency difference (14.3 cm^{-1}) between the acetone trimer and the acetone−(DMSO)$_2$ cluster shown in Table 1.[40] This is considered to be due to the fact that the ab initio MO calculations are done only for the clusters at their potential energy minima, while the thermal distributions of the molecular configurations are explicitly treated in the MD simulations of the liquid structures. At this point, it is also considered to be worth noting that, for the same reason, the vibrational frequency shift from the gas phase is calculated to be about 20 cm^{-1} for a dilute solution of acetone in DMSO (∼1717 cm^{-1} vs 1737 cm^{-1}), while the frequency difference between the isolated acetone molecule and the acetone−(DMSO)$_2$ cluster is as large as 46.7 cm^{-1} (Table 1). In other words, taking into account the mechanism given in eq 8, the electric field operating in the acetone−(DMSO)$_2$ cluster is larger than (but on the same order of magnitude as) that operating in a dilute solution of acetone in DMSO.

The calculated magnitudes of the NCE defined as $\tilde{\nu}_{NCE} \equiv \tilde{\nu}_{aniso} - \tilde{\nu}_{iso}$ are plotted in Figure 3b. The observed values taken from ref 21 are also shown for comparison. The NCE calculated for neat liquid acetone (6.2 cm^{-1}) is in reasonable agreement with the observed value (5.5 cm^{-1}). The concave curvature of the plot is also in agreement with the experimental result. As discussed in our previous study,[21] the sign of the curvature for acetone in DMSO is opposite to that for acetone in CCl_4,[14,17,41] because of the difference in the polarity between the two solvents (DMSO and CCl_4) as compared with that of acetone.[42]

The bandwidths of the observed and calculated spectra are plotted in Figure 4. The bandwidths calculated for neat liquid acetone are 13.5, 5.5, and 20.8 cm^{-1} for the IR, isotropic Raman, and anisotropic Raman bands, respectively, in agreement with the observed values (∼14, 8.5, and 20.3 cm^{-1}, respectively).[14,15] Upon dilution in DMSO, the calculated width decreases for the anisotropic Raman band and increases for the isotropic Raman band. These changes are also in agreement with the experimental results. Note that we are not using any convoluting function in the simulations of the spectra in the present study. It may be said, therefore, that the main factors that determine the bandwidths are included in the present simulations.

To examine the factors that determine the band profiles in more detail, the spectra in the static case (without the effect of liquid dynamics) are also calculated in a way as described in the last part of section 2A. The result is shown in Figure 5.

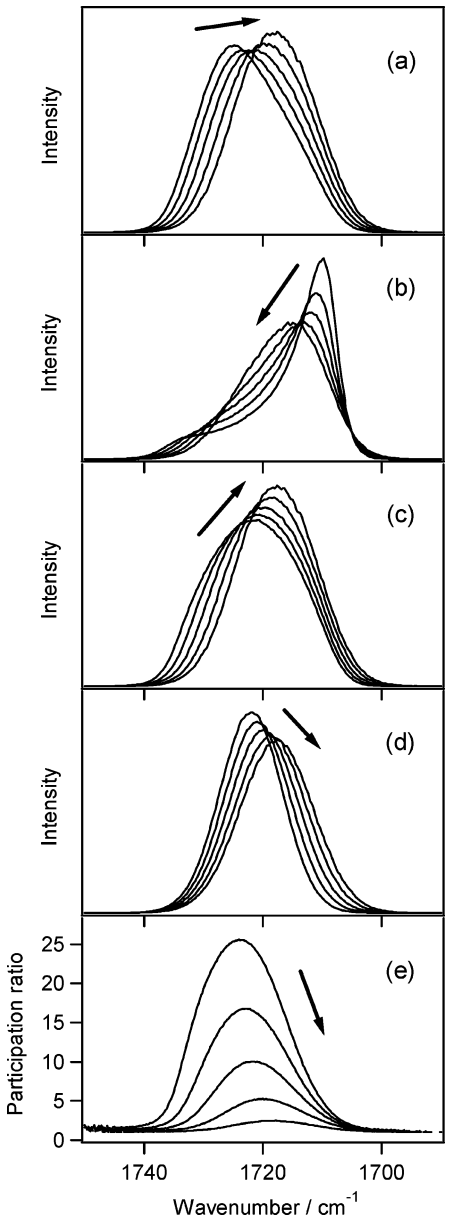

Figure 5. (a) IR, (b) isotropic Raman, and (c) anisotropic Raman spectra and (d) the spectra in the no-coupling limit of neat liquid acetone and the acetone/DMSO binary liquid mixtures in the C=O stretching region, calculated in the static case. (e) The frequency-dependent participation ratio $\eta(\omega)$, as defined in eq 9. The arrows indicate the direction of the changes upon dilution in DMSO from $x_{acetone} = 1.0$ to $x_{acetone} = 0.2$.

Compared with the spectra in Figure 2, it is clearly seen that the effect of liquid dynamics is most significant on the profile of the isotropic Raman band of neat liquid acetone. There is a small bump at $\sim$1735 cm^{-1} on this band in the static case as shown in Figure 5b, but it disappears by the effect of liquid dynamics as shown in Figure 2b. Accordingly, the asymmetry of the band profile, defined as $A = 2(\Gamma_{blue} - \Gamma_{red})/\Gamma_{full}$, where Γ_{blue} and Γ_{red} are the blue and red side half widths at half-maximum and $\Gamma_{full} = \Gamma_{blue} + \Gamma_{red}$ is the full width at half-maximum, is reduced from 0.67 in the static case [Figure 5b] to 0.29 in the dynamic case [Figure 2b]. The latter value is close to the observed value of $\sim$0.2 obtained in our previous study.[43] As expected from the motional narrowing effect of liquid dynamics, the bandwidth is also reduced from 8.2 cm^{-1} in the static case to 5.5 cm^{-1} in the dynamic case. At the lower mole fractions also, there is a similar (but less significant) effect of the liquid dynamics on the isotropic Raman band profile.

By examining the time correlation function of the diagonal terms of $H(\tau)$ (not shown), the time scale of the modulation of the diagonal terms is obtained as $\tau_f = 0.13$ ps, while the magnitude of the modulation is $\Delta_f = 5.28$ cm^{-1} (corresponding to $\Gamma_{full} = 12.4$ cm^{-1} obtained in the no-coupling limit shown in Figure 5d discussed below). Since the product $2\pi c\tau_f\Delta_f = 0.128$ is significantly smaller than unity, it is considered that the modulation of the diagonal terms of $H(\tau)$ is in the fast modulation regime.[22] This is consistent with the result that a significant change is seen in the isotropic Raman band profile as a result of liquid dynamics.

As discussed in a previous study,[4] we can see a significant difference in the bandwidth between the isotropic and anisotropic Raman bands of neat liquid acetone even in the static case (8.2 vs 20.7 cm^{-1}) as shown in Figure 5, panels b and c. This difference arises from the off-diagonal vibrational coupling. Therefore, it may be said that the major part of the difference in the bandwidth between these two bands in the dynamic case (5.5 vs 20.8 cm^{-1}) shown in Figure 2b,c also arises from the off-diagonal vibrational coupling. The broadening of the anisotropic Raman band due to the off-diagonal vibrational coupling is also seen by comparing it with the spectrum in the no-coupling limit [Figure 5d, $\Gamma_{full} = 12.4$ cm^{-1}], which is calculated by switching off all the off-diagonal vibrational coupling. In contrast, at the mole fraction of $x_{acetone} = 0.2$, the isotropic and anisotropic Raman bands have almost the same width in the static case (16.4 vs 16.0 cm^{-1}). The difference in their bandwidths in the dynamic case (8.9 vs 12.0 cm^{-1}) is therefore considered to arise from the liquid dynamics, probably from the rotational motions of acetone molecules, as expected from the theory of vibrational band shapes of dilute solutions.[44−46]

C. Extent of Delocalization of Vibrational Motions. As discussed in a previous study,[23] the diagonal and off-diagonal effects compete with each other in determining the extent of delocalization of vibrational modes. Since we have obtained a good agreement between the observed and calculated spectral features, it is considered to be meaningful to examine the extent of delocalization of vibrational motions that give rise to those spectral features. One way to estimate the extent of delocalization is to calculate the frequency-dependent participation ratio, defined as

TABLE 2: Extent of Delocalization of the C=O Stretching Mode of Acetone in Acetone/DMSO Binary Liquid Mixtures

						extent of delocalization			
$x_{acetone}$	$\tilde{\nu}_{NCE}$/cm^{-1}	Γ_{iso}/cm^{-1}	D_{iso}	Γ_{aniso}/cm^{-1}	D_{aniso}	from D_{iso}	from D_{aniso}	max$\{\eta(\omega)\}$	$d(t)$ at $t = 6$ ps
1.0	6.22	5.49	2.67	20.78	0.70	>130	45	25.6	43.3
0.8	4.57	6.35	1.70	18.48	0.58	110	30	16.8	25.1
0.6	3.20	7.68	0.98	16.42	0.46	60	18	10.1	13.7
0.4	1.96	8.85	0.52	14.28	0.32	22	9	5.3	6.3
0.2	0.93	8.86	0.25	11.99	0.18	6	3	2.5	2.9

$$\eta(\omega) = \frac{\left\langle \sum_{\xi=1}^{N} \left(\sum_{j=1}^{N} c_{j\xi}{}^{4} \right)^{-1} \delta(\omega - \omega_{\xi}) \right\rangle}{\left\langle \sum_{\xi=1}^{N} \delta(\omega - \omega_{\xi}) \right\rangle} \tag{9}$$

where $c_{j\xi}$ is the normalized vibrational amplitude of the jth molecule in the ξth mode, ω_{ξ} is the vibrational frequency of the ξth mode, and N is the number of molecules in the system (which is equal to the number of modes). This quantity represents the average extent of delocalization of the modes at the specified frequency, and is equal to 1 if the modes at the specified frequency are completely localized, and equal to n if they are uniformly delocalized over n molecules.[47−50] The result is shown in Figure 5e. The value of $\eta(\omega)$ is large around the band center and small on the wing in the same way as the model liquid system treated in ref 23, and the peak height becomes lower upon dilution in DMSO. This peak height, denoted as $\max\{\eta(\omega)\}$, is summarized in the ninth column in Table 2.

It has been discussed[23] that the peak height of $\eta(\omega)$ is related to the quantity called NCE detectability, which is defined as the ratio between the magnitude of NCE and the bandwidth. In the fourth and sixth columns of Table 2, the values of NCE detectability, calculated as $D_{\mathrm{iso}} = z\,\tilde{\nu}_{\mathrm{NCE}}/\Gamma_{\mathrm{iso}}$ and $D_{\mathrm{aniso}} = z\,\tilde{\nu}_{\mathrm{NCE}}/\Gamma_{\mathrm{aniso}}$ with $z = 2\sqrt{2\ln 2}$, are shown. By employing the relation shown in Figure 4 of ref 23, the extent of delocalization has been estimated from these values as shown in the seventh and eighth columns of Table 2. It is seen that the extent of delocalization estimated from D_{aniso} is in reasonable agreement with $\max\{\eta(\omega)\}$ directly obtained from the present simulations. This result means that, although the relation between $\max\{\eta(\omega)\}$ and D_{aniso} shown in Figure 4 of ref 23 is obtained for a model liquid system, it is also applicable to a real liquid system. In other words, the present result supports the idea[23] that the extent of delocalization of vibrational motions is related to observable features of the Raman band profiles. In contrast, the extent of delocalization estimated from D_{iso} is too large as compared with the true values of $\max\{\eta(\omega)\}$, especially at large mole fractions of acetone. This is considered to be due to the motional narrowing effect on the isotropic Raman band profiles, which is not taken into account in the calculations for the model liquid system treated in ref 23. In fact, since $\eta(\omega)$ is based on the instantaneous normal modes as seen in eq 9, it does not include any effect of the time dependence of the vibrational Hamiltonian by definition.

Another way to estimate the extent of delocalization is to examine the time evolution of locally excited vibrations. From the quantity defined as

$$z_{kj}(t) = \left\langle x_k \middle| \exp_{+}\left[-\frac{i}{\hbar} \int_0^t \mathrm{d}\tau\, H(\tau) \right] \middle| x_j \right\rangle \tag{10}$$

where $|x_j\rangle$ is the normalized vibrational wave function locally excited on the jth molecule, the extent of delocalization after time t is calculated as

$$d(t) = \left\langle \frac{1}{N} \sum_{j=1}^{N} \left(\sum_{k=1}^{N} |z_{kj}(t)|^{4} \right)^{-1} \right\rangle \tag{11}$$

In the same way as $\eta(\omega)$ defined in eq 9, $d(t)$ is equal to 1 if the vibrational wave functions remain totally localized, and equal to n if they are uniformly delocalized over n molecules. In contrast to $\eta(\omega)$, $d(t)$ includes all the effects of the time dependence of the vibrational Hamiltonian $H(t)$, especially the time-dependent modulation of the diagonal force constants that give rise to broadening and narrowing of band profiles. The result is shown in Figure 6. It is seen that the initially localized vibrational excitations become delocalized as time evolves, and the speed of delocalization is faster at higher mole fractions of acetone. Taking into account that the vibrational population lifetime of the C═O stretching mode of acetone is about 6 ps,[51] we show the values of $d(t)$ at $t = 6$ ps in the last column in Table 2. It is easily recognized that the changes in the values of $d(t)$ at $t = 6$ ps as a function of mole fraction are parallel to those of $\max\{\eta(\omega)\}$.

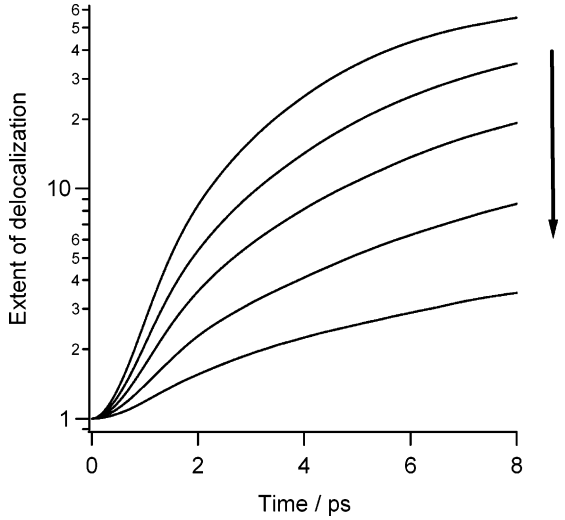

Figure 6. The time evolution of the extent of delocalization of the initially localized vibrational excitations, as defined in eq 11. The arrow indicates the direction of the change upon dilution in DMSO from $x_{\mathrm{acetone}} = 1.0$ to 0.2.

The above results demonstrate that, in the acetone/DMSO binary liquid mixture of $x_{\mathrm{acetone}} = 0.2$, the vibrational wave functions of the C═O stretching mode are delocalized over only 2 or 3 molecules, but in neat liquid acetone they are delocalized over a few tens of molecules. Considering that the extent of delocalization is related to the NCE detectability, it may be said that the vibrational band profiles of neat liquid acetone are controlled by the structure and dynamics over a length scale a few times longer than the molecular scale. In other systems also, vibrational bands with a similar value of NCE detectability (such as the amide I band of liquid formamide[52]) are expected to contain information on the structure and dynamics over such a long length scale. We suggest that this aspect of the relation between the vibrational motions and vibrational spectroscopic features is important for the correct understanding of intermolecular vibrational interactions and intermolecular vibrational excitation transfer in the liquid phase.

4. Summary

In the present study, the MD/TDC/WFP method[26] has been extended to include the variation of the diagonal terms of the time-dependent vibrational Hamiltonian by the electric field from the surrounding molecules according to eq 8. This method is then applied to the C═O stretching band of neat liquid acetone and the acetone/DMSO binary liquid mixtures, and the concentration dependence of the NCE, the diagonal frequency shifts, and the extent of delocalization has been studied. To specify the mechanism of the diagonal frequency shifts, ab initio MO calculations have also been carried out for the acetone trimer and the acetone−$(\mathrm{DMSO})_2$ cluster.

The main conclusions obtained from the calculations may be summarized as follows. (1) The diagonal frequency shifts of the C═O stretching mode calculated for the acetone trimer and the acetone−$(DMSO)_2$ cluster by the ab initio MO method are reasonably well explained by using eq 8. This result suggests that the diagonal frequency shifts of the C═O stretching mode of acetone arising from the interactions with the surrounding acetone and DMSO molecules are controlled by the electric field from those surrounding molecules. From the comparison with the calculations by the SCRF method, it has also been suggested that the molecular aspect of the solvent effect is important for those frequency shifts. (2) In the spectra calculated by the extended MD/TDC/WFP method, the anisotropic Raman band shows a large low-frequency shift while the isotropic Raman band shows only a small frequency shift upon dilution in DMSO, in agreement with the experimental result.[21] The experimentally observed downward curvature of the concentration dependence of the NCE[21] is also well reproduced by the simulations. (3) The widths of the IR, isotropic Raman, and anisotropic Raman bands of neat liquid acetone are calculated as 13.5, 5.5, and 20.8 cm^{-1}, respectively, in good agreement with the observed values (∼14, 8.5, and 20.3 cm^{-1}, respectively).[14,15] Upon dilution in DMSO, the calculated width decreases for the anisotropic Raman band and increases for the isotropic Raman band, also in agreement with the experimental result. A detailed examination of the factors that determine these bandwidths indicates that the band broadening due to the diagonal and off-diagonal effects and the motional narrowing due to the liquid dynamics are both important. (4) The extent of delocalization of the C═O stretching mode is strongly dependent on the mole fraction of the liquid mixtures, and is related to the quantity called NCE detectability. In the case of neat liquid acetone, the C═O stretching vibrations are delocalized over a few tens of molecules, indicating that the vibrational band profiles of neat liquid acetone are controlled by the structure and dynamics over a length scale a few times longer than the molecular scale.

The calculations in the present study demonstrate that, by using the extended MD/TDC/WFP method, it is possible to examine the vibrational spectroscopic features arising from the diagonal and off-diagonal effects and the influence of liquid dynamics for vibrational modes with large dipole derivatives. It therefore helps to elucidate the relation between the features of vibrational band profiles and the behavior of the vibrational excitation transfer in the liquid phase.

Acknowledgment. Part of this study was carried out as a joint research project within the Japan-Austria Research Cooperative Program. The financial support by the Japan Society for the Promotion of Science (JSPS) to H.T. and by FWF as project P16372-N02 to M.M. is gratefully acknowledged. The Italian MIUR is acknowledged (by M.G.G. and M.M.) for financial support to part of this work within the FIRB project "Molecular dynamics in complex liquids".

References and Notes

(1) Torii, H. *Vib. Spectrosc.* **2002**, *29*, 205.
(2) McHale, J. L. *J. Chem. Phys.* **1981**, *75*, 30.
(3) Logan, D. E. *Chem. Phys.* **1986**, *103*, 215.
(4) Torii, H.; Tasumi, M. *J. Chem. Phys.* **1993**, *99*, 8459.
(5) Hush, N. S.; Williams, M. L. *J. Mol. Spectrosc.* **1974**, *50*, 349.
(6) Bishop, D. M. *J. Chem. Phys.* **1993**, *98*, 3179.
(7) Hush, N. S.; Reimers, J. R. *J. Phys. Chem.* **1995**, *99*, 15798.
(8) Andrews, S. S.; Boxer, S. G. *J. Phys. Chem. A* **2002**, *106*, 469.
(9) Ham, S.; Cho, M. *J. Chem. Phys.* **2003**, *118*, 6915.
(10) Torii, H. *J. Phys. Chem. A* **2004**, *108*, 7272.
(11) Fini, G.; Mirone, P. *J. Chem. Soc., Faraday Trans. 2* **1974**, *70*, 1776.
(12) Schindler, W.; Sharko, P. T.; Jonas, J. *J. Chem. Phys.* **1982**, *76*, 3493.
(13) Dybal, J.; Schneider, B. *Spectrochim. Acta A* **1985**, *41*, 691.
(14) Musso, M.; Giorgini, M. G.; Döge, G.; Asenbaum, A. *Mol. Phys.* **1997**, *92*, 97.
(15) Bertie, J. E.; Michaelian, K. H. *J. Chem. Phys.* **1998**, *109*, 6764.
(16) Torii, H. In *Novel Approaches to the Structure and Dynamics of Liquids*: *Experiments, Theories and Simulations*; Samios, J., Durov, V. A., Eds.; Kluwer: Dordrecht, The Netherlands, 2004; p 343.
(17) Giorgini, M. G.; Fini, G.; Mirone, P. *J. Chem. Phys.* **1983**, *79*, 639.
(18) Kamoun, M.; Mirone, P. *Chem. Phys. Lett.* **1980**, *75*, 287.
(19) Musso, M.; Giorgini, M. G.; Torii, H.; Dorka, R.; Schiel, D.; Asenbaum, A.; Keutel, D.; Oehme, K.-L. *J. Mol. Liq.* In press.
(20) Logan, D. E. *Mol. Phys.* **1986**, *58*, 97.
(21) Giorgini, M. G.; Musso, M.; Torii, H. *J. Phys. Chem. A* **2005**, *109*, 5846.
(22) Kubo, R. *Adv. Chem. Phys.* **1969**, *15*, 101.
(23) Torii, H. *J. Phys. Chem. A* **2004**, *108*, 2103.
(24) Woutersen, S.; Bakker, H. J. *Nature* **1999**, *402*, 507.
(25) Seifert, G.; Zürl, R.; Patzlaff, T.; Graener, H. *J. Chem. Phys.* **2000**, *112*, 6349.
(26) Torii, H. *J. Phys. Chem. A* **2002**, *106*, 3281.
(27) Mukamel, S. *Principles of Nonlinear Optical Spectroscopy*; Oxford University Press: New York, 1995.
(28) Torii, H. *J. Chem. Phys.* **2003**, *119*, 2192.
(29) In the present paper, we frequently use atomic units. E_h is the Hartree energy, a_0 is the Bohr radius, and m_e is the electron mass.
(30) Bayliss, N. S.; Cole, A. R. H.; Little, L. H. *Aust. J. Chem.* **1955**, *8*, 26.
(31) Jorgensen, W. L.; Briggs, J. M.; Contreras, M. L. *J. Phys. Chem.* **1990**, *94*, 1683.
(32) Luzar, A.; Soper, A. K.; Chandler, D. *J. Chem. Phys.* **1993**, *99*, 6836.
(33) Evans, D. J. *Mol. Phys.* **1977**, *34*, 317.
(34) Allen, M. P.; Tildesley, D. J. *Computer Simulation of Liquids*; Oxford University Press: Oxford, UK, 1989.
(35) *Handbook of Chemistry and Physics*, 85th ed.; CRC Press: Boca Raton, FL, 2004/2005.
(36) *The Merck Index*, 13th ed.; Merck Research Laboratories, 2001.
(37) Frisch, M. J.; Trucks, G. W.; Schlegel, H. B.; Scuseria, G. E.; Robb, M. A.; Cheeseman, J. R.; Zakrzewski, V. G.; Montgomery, J. A., Jr.; Stratmann, R. E.; Burant, J. C.; Dapprich, S.; Millam, J. M.; Daniels, A. D.; Kudin, K. N.; Strain, M. C.; Farkas, O.; Tomasi, J.; Barone, V.; Cossi, M.; Cammi, R.; Mennucci, B.; Pomelli, C.; Adamo, C.; Clifford, S.; Ochterski, J.; Petersson, G. A.; Ayala, P. Y.; Cui, Q.; Morokuma, K.; Malick, D. K.; Rabuck, A. D.; Raghavachari, K.; Foresman, J. B.; Cioslowski, J.; Ortiz, J. V.; Baboul, A. G.; Stefanov, B. B.; Liu, G.; Liashenko, A.; Piskorz, P.; Komaromi, I.; Gomperts, R.; Martin, R. L.; Fox, D. J.; Keith, T.; Al-Laham, M. A.; Peng, C. Y.; Nanayakkara, A.; Gonzalez, C.; Challacombe, M.; Gill, P. M. W.; Johnson, B. G.; Chen, W.; Wong, M. W.; Andres, J. L.; Head-Gordon, M.; Replogle, E. S.; Pople, J. A. *Gaussian 98*, Gaussian, Inc.: Pittsburgh, PA, 1998.
(38) Wong, M. W.; Frisch, M. J.; Wiberg, K. B. *J. Am. Chem. Soc.* **1991**, *113*, 4776.
(39) Park, E. S.; Boxer, S. G. *J. Phys. Chem. B* **2002**, *106*, 5800.
(40) Strictly speaking, the frequency difference (14.3 cm^{-1}) between the acetone trimer and the acetone−$(DMSO)_2$ cluster in Table 1 should be compared with the frequency shift of the ^{13}C species, which is almost free from the off-diagonal vibrational coupling. However, the comparison described in the text is valid because there is essentially no frequency shift due to the off-diagonal effect for the anisotropic Raman band.
(41) Torii, H.; Musso, M.; Giorgini, M. G.; Döge, G. *Mol. Phys.* **1998**, *94*, 821.
(42) Logan, D. E. *Chem. Phys.* **1989**, *131*, 199.
(43) Musso, M.; Torii, H.; Giorgini, M. G.; Döge, G. *J. Chem. Phys.* **1999**, *110*, 10076.
(44) Gordon, R. G. *J. Chem. Phys.* **1965**, *43*, 1307.
(45) Rothschild, W. G.; Rosasco, G. J.; Livingston, R. C. *J. Chem. Phys.* **1975**, *62*, 1253.
(46) Oxtoby, D. W. *Adv. Chem. Phys.* **1979**, *40*, 1.
(47) Bell, R. J.; Dean, P. *Discuss. Faraday Soc.* **1970**, *50*, 55.
(48) Thouless, D. J. *Phys. Rep.* **1974**, *13*, 93.
(49) Weaire, D.; Williams, A. R. *J. Phys. C*: *Solid State Phys.* **1977**, *10*, 1239.
(50) Evensky, D. A.; Scalettar, R. T.; Wolynes, P. G. *J. Phys. Chem.* **1990**, *94*, 1149.
(51) Ge, N.-H.; Zanni, M. T.; Hochstrasser, R. M. *J. Phys. Chem. A* **2002**, *106*, 962.
(52) Mortensen, A.; Faurskov Nielsen, O.; Yarwood, J.; Shelley, V. *J. Phys. Chem.* **1994**, *98*, 5221.